ELSEVIER

Journal of Biomechanics 41 (2008) 1659–1667

JOURNAL OF BIOMECHANICS

www.elsevier.com/locate/jbiomech
www.JBiomech.com

NMClab, a model to assess the contributions of muscle visco-elasticity and afferent feedback to joint dynamics

Alfred C. Schouten[a,b,*], Winfred Mugge[a], Frans C.T. van der Helm[a,b]

[a]*Department of Biomechanical Engineering, Faculty of Mechanical Engineering, Laboratory for Neuromuscular Control, Delft University of Technology, Mekelweg 2, 2628 CD Delft, The Netherlands*

[b]*Institute for Biomedical Technology (BMTI), Laboratory of Biomechanical Engineering, University of Twente, P.O. Box 217, 7500 AE Enschede, The Netherlands*

Accepted 16 March 2008

Abstract

The dynamic behavior of a neuromusculoskeletal system results from the complex mechanical interaction between muscle visco-elasticity resulting from (co-)contraction and afferent feedback from muscle spindles and Golgi tendon organs. As a result of the multiple interactions the individual effect of each of the structures to the overall dynamics is hard to recognize, if not impossible. Here a neuromuscular control (NMC) model is developed to analyze the functional contribution of the various physiological structures on the mechanical behavior of a limb. The dynamics of a joint are presented in admittances, i.e. the dynamic relation between input force (or torque) and the output displacement, which can be represented by either frequency or impulse response functions. With the model it can be shown that afferent feedback reduces, while muscle visco-elasticity increases, the stability margins. This implicates that there is a delicate balance between muscle co-contraction and afferent feedback, which depends on the joint specific physiological properties. The main application of the model is educational; it is implemented in a graphical user interface allowing users to explore the role of the various physiological structures on joint dynamics. Other applications of the model are more experimental, e.g. to elucidate experimentally measured admittances and to compare the quantified parameter values with the theoretically optimal ones. It is concluded that the NMC model is a useful and intuitive tool to investigate human motor control, in a theoretical as well as an experimental way.

Keywords: Neuromuscular control; Afferent feedback; Reflexes; Model

1. Introduction

The human motor control system involves a complex mechanical interaction between limbs, muscles, tendons, afferent feedback and the central nervous system (CNS). Major sources of afferent feedback are muscle force feedback by Golgi tendon organs and stretch (including stretch velocity) feedback by muscle spindles. Both pathways contribute to the dynamics of a joint. As a result of many nested feedback loops present in the human motor control system the effect of each component is difficult to predict, if not impossible, especially as multiple interactions exist. The goal of this study was to develop a model to allow for assessment of the effect of the individual components and their interactions on total joint dynamics.

Experimental studies have shown that the reflexive contribution from afferents to the joint dynamics can be of the same order of magnitude as the intrinsic muscular contribution (Sinkjaer et al., 1988; Kearney et al., 1997; van der Helm et al., 2002; de Vlugt et al., 2002; Schouten et al., 2008b). It is known that the reflex magnitude varies with stretch amplitude, muscle activation level (Kearney and Hunter, 1983, 1984; Stein and Kearney, 1995), perturbation bandwidth and the dynamics of an external load (van der Helm et al., 2002; de Vlugt et al., 2002; Schouten et al., 2008b). Theoretical studies showed that

*Corresponding author at: Department of Biomechanical Engineering, Faculty of Mechanical Engineering, Laboratory for Neuromuscular Control, Delft University of Technology, Mekelweg 2, 2628 CD Delft, The Netherlands. Tel.: +31 15 278 5247.

E-mail address: a.c.schouten@tudelft.nl (A.C. Schouten).

URL: http://www.3me.tudelft.nl/nmc (A.C. Schouten).

0021-9290/$ - see front matter © 2008 Elsevier Ltd. All rights reserved.
doi:10.1016/j.jbiomech.2008.03.014

these reflex modulations were optimal to suppress the displacement, suggesting that in human motor control the CNS acts as an optimal controller (Schouten et al., 2001; de Vlugt et al., 2002).

Reflex modulation has been shown during experiments, although the origin of these adaptations is unclear and often debated (Loeb, 1987). In biology many physiological phenomena contribute to the afferent feedback gain. Basically four global structures can be recognized in the afferent feedback loop: the receptor, the afferent, the motoneuron pool, and the muscle. Stein and Capaday (1988) showed that during walking the strength of the H-reflex varied (Stein and Capaday, 1988). The authors suggested that the observed modulation resulted from modulating presynaptic inhibition of Ia afferents. Another phenomenon that contributes to the loop gain is γ-motoneurons. γ-Motoneurons activate the intrafusal muscle fibers in the muscle spindles and as such adjust the sensitivity of the muscle spindles. Afferent feedback is integrated with the tonic descending input of higher centers of the CNS (for co-contraction) at the α-motoneurons. Both presynaptic inhibition and post-activation depression affect afferent feedback (Hultborn et al., 1996; Voigt and Sinkjaer, 1998; Rudomin and Schmidt, 1999; Nielsen et al., 2007). Likely all mentioned phenomena have an impact on the afferent feedback loop, suggesting that the CNS adapts while taking into account all phenomena.

It is well known that the human motor control system is non-linear, e.g. the sensitivity of muscle spindles is unidirectional (Kearney et al., 1997). This has led to studies following non-linear approaches to studying the human motor control system (Kearney et al., 1997; Zhang and Rymer, 1997). Other researchers used linear techniques under specific conditions: the human motor control system behaves quasi-linear in many postural conditions or can be linearized around an operating point as long as the displacements are small (de Vlugt et al., 2002; Kearney and Hunter, 1984). The merit of a linear approach is that many useful tools are available for linear systems, e.g. analysis of stability. In this study a model is developed with an educational purpose. To enable the use of these tools the presented model is linear and therefore describes the human motor control behavior in postural conditions. The model incorporates both the musculoskeletal and afferent/reflexive contributions to joint dynamics and therefore includes a limb (inertia), visco-elastic properties of (co-contracted) muscles, tendon elasticity and afferent feedback from Golgi tendon organs and muscle spindles. The presented model is unique as it includes all relevant physiological mechanisms allowing analysis of the interaction between these mechanisms. The presented model is made freely available in software allowing users to explore the interactions through an intuitive, easily interpretable, graphical user interface.[1] Other applications of the model are more experimental: experimentally obtained admittances can be compared to modeled admittances to find the underlying physical parameters, assess whether the given settings result in optimal performance, and analyze the sensitivity of the admittance to parameter variations.

2. Method

2.1. Model

The model describes the dynamics of a human joint, which may be in interaction with an external environment, or load. The model is based on experimental measurements of the human shoulder (van der Helm et al., 2002; de Vlugt et al., 2002; Schouten et al., 2008b). In these experiments the subjects were instructed to minimize the displacements while continuous force perturbations were applied by a manipulator via a handle, see Fig. 1. Force perturbations, in contrast to position perturbations, enable subjects to directly influence the displacements and allow for natural task performance: the subject must actively control the position and preserve stability. Such postural control tasks allow for a linear approach to motor control enabling the use of linear control engineering tools, i.e. the admittance of the limb is described in frequency domain by a frequency response function (FRF). An FRF can graphically be displayed in a Bode diagram. The same information can also be assessed from the impulse response function (IRF) of the admittance. The IRF is obtained by inverse Fourier transforming the FRF.

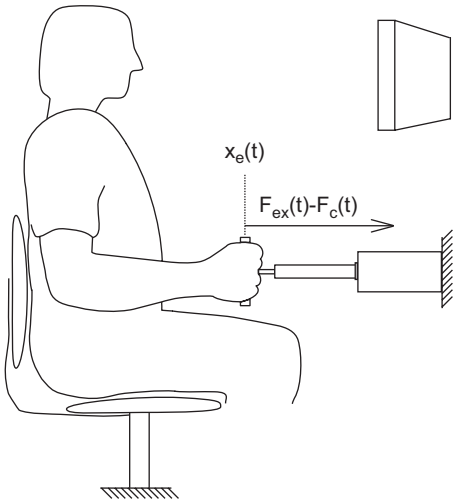

Fig. 1. Experimental set-up; the subject was seated on a chair and held the handle with the right hand. The subject could move the handle for- and backwards. The interaction force $F_c(t)$ was measured by a force transducer mounted between the handle and the piston of the hydraulic manipulator. The manipulator controlled the position of the handle $x_e(t)$, based on the human reaction force $F_c(t)$, the external force perturbation $F_{ex}(t)$ and the simulated external load (also environment). The subject controlled the position of the handle in face of external force perturbations. To motivate the subject and to prevent drift the actual position of the handle and the reference position were shown on the display.

[1]The model, NMClab, is implemented in Matlab (The Mathworks, Inc., Natick, MA) and is available on http://www.3me.tudelft.nl/nmc.

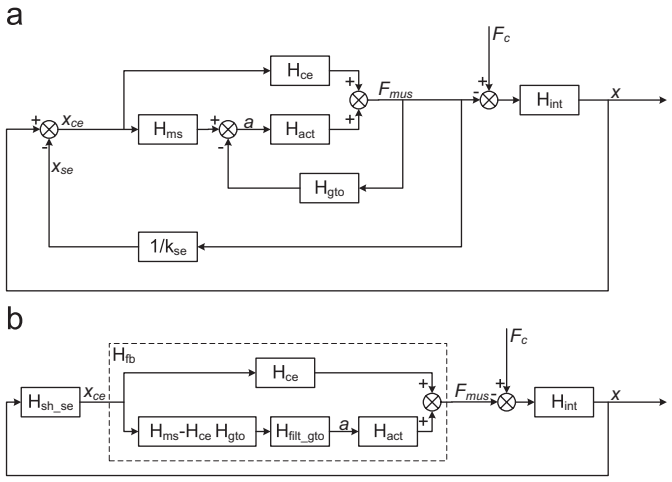

Fig. 2. Representations of the neuromusculoskeletal model. Model A denotes the model of a human joint as used in this study. For the derivation of the formulae an alternative representation of the block scheme was used which is presented in B. The derivations are discussed in the text; the signals are summarized in Table 1.

Table 1
Description of the signals used in the model

Signal	Description
F_{ex} (N)	External force
F_c (N)	Reaction force at contact (i.e. the handle)
F_{mus} (N)	Muscle force
a (N)	Muscle activation
x_e (m)	Endpoint displacements (handle)
x (m)	Joint position
x_{ce} (m)	Length contractile element
x_{se} (m)	Length series elastic element

A block scheme of the model is shown in Fig. 2A. In accordance with the experimental studies, all signals are expressed at endpoint level, i.e. the hand, in one degree-of-freedom (1-DoF) and, since it is a (control) engineering model, as deviations around their mean. The signals are summarized in Table 1. The equations were derived from the block scheme, and the expressions are given in Appendix A (Bobet and Norman, 1990; Olney and Winter, 1985; Potvin et al., 1996; Stroeve, 1999). The description of all the parameters and default values for the shoulder joint are summarized in Table 2.

The limb (H_{int}) is described by a mass and passive visco-elasticity from e.g. surrounding tissues. The displacements of the joint (x) result from the net force acting on the limb, i.e. the reaction force at the handle (F_c) and the muscle force (F_{mus}). The muscle force includes the muscle visco-elasticity of all muscles (H_{ce}) resulting from tonic (co)-contraction and additional (phasic) muscle activation (a), resulting from afferent feedback. The built-up of muscle force is described by the muscle activation dynamics (H_{act}). Considering relatively small displacements, the total length of the muscle complex is proportional to the position of the limb (x). The contractile element of the muscle (x_{ce}) is in series with the tendon (x_{se}). The tendon, i.e. the series elastic element, is represented by a tendon elasticity (k_{se}).

Table 2
Description of the model parameters and default values describing the human shoulder

Parameter	Default value	Description
m	2 kg	Mass/inertia arm
b	30 Ns/m	Muscle viscosity
k	400 N/m	Muscle elasticity
b_q	0 Ns/m	Passive viscosity
k_q	0 N/m	Passive elasticity
f_0	2.5 Hz	Bandwidth, activation dynamics
β	0.7 –	Relative damping, activation dynamics
k_{se}	10 kN/m	Tendon elasticity
k_a	0 Ns^2/m	Acceleration feedback gain
k_v	30 Ns/m	Velocity feedback gain
k_p	0 N/m	Position feedback gain
k_f	0 –	Force feedback gain
τ_d	25 ms	Neural time delay
b_c	200 Ns/m	Contact viscosity
k_c	12 kN/m	Contact elasticity
m_e	1 kg	Mass/inertia environment
b_e	0 Ns/m	Damping environment
k_e	0 N/m	Stiffness environment

The parameters are based on experimental studies (van der Helm et al., 2002; de Vlugt et al., 2002; Schouten et al., 2008b).

The α-motoneuron pool at the spinal cord integrates all afferent feedback and is represented as a summation (the summation point between the blocks with H_{ms} and H_{act}). No dynamics representing spinal cord circuitry are included as its dynamics are much faster than the other dynamics in the loop. All spinal feedback pathways originating from the muscle spindles are represented in the muscle spindle feedback (H_{ms}). In biological systems the major contributors are the monosynaptic stretch reflex and reciprocal inhibition. Muscle spindles are positioned parallel to the muscle fibers and consequently they are sensitive to stretch and stretch velocity of the contractile element of the muscle. Some studies suggested that muscle spindles are also sensitive to the second order derivative, i.e. stretch acceleration. The Golgi tendon organs (H_{gto}) are sensitive to the force in the tendon. By the convention used in the present model muscle spindles excite and Golgi tendon organs inhibit the motoneuron pool. However, in the model it is possible to set feedback gains to negative values; effectively changing inhibitory to excitatory, and vice versa. All time delays present in the reflexive feedback loops, i.e. the afferent and the efferent pathway, are lumped in one neural time delay. For simplicity it is assumed that the neural time delay for the muscle spindle and Golgi tendon organ feedback loop are equal.

2.2. Closing the loops

The model in Fig. 2A is rearranged to the one in Fig. 2B and an environment is added, including contact dynamics,

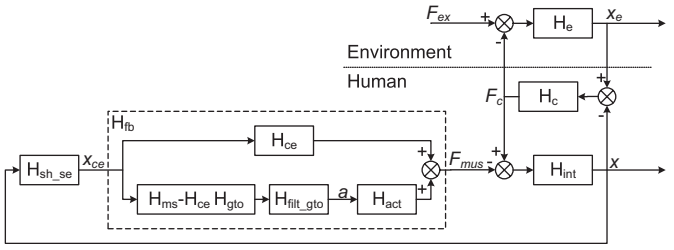

Fig. 3. Representation of the neuromusculoskeletal model in frequency domain supplemented with an environment. An environment is coupled to the human joint model from Fig. 2B. The model derivation is discussed in the text; the signals are summarized in Table 1.

to finally form the model in Fig. 3. Details of the rearrangement from Fig. 2A–B are given in Appendix A.

2.2.1. Intrinsic and afferent feedback

First the feedback loop formed by the Golgi tendon organs is split into two feedback loops; one loop around the activation dynamics and one loop parallel to the muscle spindle, see Fig. C.1 in Appendix A (in the Supplement). Effectively the feedback loop of the Golgi tendon organs around the activation dynamics acts as a filter on the activation dynamics (H_{filtgto}):

$$H_{\mathrm{filtgto}} = \frac{1}{1 + H_{\mathrm{act}} H_{\mathrm{gto}}} \tag{1}$$

The reactive muscle force as a result of the displacements (H_{fb}) can be divided into two parallel pathways: intrinsic feedback, i.e. the visco-elastic properties of the active (co-contracted) muscles, and afferent/reflexive feedback from muscle spindles and Golgi tendon organs, see Fig. 2B:

$$H_{\mathrm{fb}} = \frac{F_{\mathrm{mus}}}{x_{\mathrm{ce}}} = H_{\mathrm{ce}} + (H_{\mathrm{ms}} - H_{\mathrm{ce}} H_{\mathrm{gto}}) H_{\mathrm{filtgto}} H_{\mathrm{act}} \tag{2}$$

The first term in the above equation represents the muscle visco-elasticity. The remaining part is the result from afferent feedback and includes (1) the muscle spindle feedback, (2) the effect of the Golgi tendon organ feedback on the muscle visco-elasticity, (3) the filtering effect of the Golgi tendon organ on the activation dynamics, and (4) the muscle activation dynamics itself.

2.2.2. The interaction with the tendon

Fig. 2B includes a rearrangement of the tendon elasticity loop. As a result of tendon elasticity the displacement of the joint is not proportional to the length of the muscle contractile element, represented in the shaping effect of the tendon (H_{shse}):

$$H_{\mathrm{shse}} = \frac{x_{\mathrm{ce}}}{x} = \frac{k_{\mathrm{se}}}{k_{\mathrm{se}} + H_{\mathrm{fb}}} \tag{3}$$

Note that when the tendon is assumed infinitely stiff, H_{shse} equals one and the effect is not present.

2.2.3. Joint dynamics

The dynamic relation between the contact force acting on the limb and the resulting displacements of the limb are described by the mechanical admittance of the limb (H_{fx}). The reflexive impedance (H_{xa}) is defined as the variations in muscle activation related to the displacements of the limb (Schouten et al., 2008a):

$$H_{fx} = \frac{x}{F_{\mathrm{c}}} = \frac{H_{\mathrm{int}}}{1 + H_{\mathrm{int}} H_{\mathrm{shse}} H_{\mathrm{fb}}} \tag{4}$$

$$H_{xa} = \frac{a}{x} = H_{\mathrm{shse}} (H_{\mathrm{ms}} - H_{\mathrm{ce}} H_{\mathrm{gto}}) H_{\mathrm{filtgto}} \tag{5}$$

The reflexive impedance is a direct measure for afferent feedback. The only differences with the afferent contribution to the feedback (right part of Eq. (2)) are the activation dynamics (H_{act}) and the filtering effect of the tendon (H_{shse}). The muscle activation (a) and consequently the reflexive impedance can be experimentally determined from EMG of relevant muscles (Schouten et al., 2008a, b).

2.2.4. Interaction with the environment

In many daily situations humans are interacting with their environment, e.g. through tools, steering wheels, etc. In Fig. 3 an environment is added to the model, including the contact dynamics. In the model the environment (H_{e}) is described by a mass-spring-damper system. One can never have infinitely stiff contact with the environment, therefore contact dynamics (visco-elasticity: H_{c}) will exist (e.g. the grip of the hand), which acts as an interface between the limb and the environment.

The combined admittance (H_{dx}) describes the mechanical interaction between limb, environment and contact. As the contact dynamics are attributed to the human (tissue deformation), it is added to the mechanical admittance of the limb (H_{xf}) first.

$$H_{xf} = \frac{F_{\mathrm{c}}}{x_{\mathrm{e}}} = \frac{H_{\mathrm{c}}}{1 + H_{\mathrm{c}} H_{fx}} \tag{6}$$

$$H_{dx} = \frac{x_{\mathrm{e}}}{F_{\mathrm{ex}}} = \frac{H_{\mathrm{e}}}{1 + H_{\mathrm{e}} H_{xf}} \tag{7}$$

Note that as a result of the contact dynamics, the displacements of the environment, i.e. the handle, are not equal to the displacements of the limb, while in most experimental set-ups the displacements of the manipulator are used for system identification (e.g. Schouten et al., 2008b).

2.3. Performance measure

When the subject is given a position task (minimize the displacements) it is beneficial to increase the joint stiffness i.e. to make the admittance small. This can mathematically be formulated as minimizing the variance of the displacements (Schouten et al., 2001)

$$J_x = \sigma_x^2 = \int_{-\infty}^{\infty} S_{xx}(f)\,\mathrm{d}f = 2\int_0^{\infty} |H_{dx}(f)|S_{dd}(f)\,\mathrm{d}f \qquad (8)$$

This performance measure (J_x) depends on both the admittance and the power spectral density of the external force perturbation (S_{dd}). A smaller value of J_x denotes smaller displacements and therefore, in case of a position task, improved performance. The 'optimal' afferent feedback depends on the external loading as it is part of the admittance. In case the force perturbation is white noise ($S_{dd}(f) = c$ for all f) the performance measure reduces to

$$J_x = 2c\int_0^{\infty} |H_{dx}(f)|\,\mathrm{d}f \qquad (9)$$

where c is a constant of an arbitrary value. Note that the performance measure J_x is only applicable when the system is stable, see Appendix B (Friedland, 1986) for the stability analysis.

3. Results

In this section the effect of parameter variations and the interactions between the afferent feedback loops onto the joint dynamics are evaluated.

3.1. Muscle visco-elasticity

Fig. 4 shows the mechanical admittance of the joint (H_{fx}) using the default parameter values as given in Table 2. Co-activation of antagonistic muscles increases both muscle viscosity and muscle elasticity. With increasing muscle elasticity the mechanical admittance decreases for the lower frequencies whereas it increases around the eigenfrequency due to oscillations. However, oscillations are damped by increasing the muscle viscosity. In general, muscle visco-elasticity increases performance and muscle viscosity reduces oscillations as it increases stability margins.

3.2. Afferent feedback

3.2.1. Muscle spindle feedback

The mechanical admittance decreases with afferent velocity feedback for frequencies below the eigenfrequency, while the static gain (gain at 0 Hz) remains equal (Fig. 5). As a result of the increased afferent feedback and the neural time delay present in the afferent feedback loop an oscillatory peak emerges at the eigenfrequency. The IRFs in Fig. 6 shows these oscillations even better. Increasing the afferent feedback gain further and further would ultimately result in an unstable system.

Muscle spindle feedback has a strong impact on the performance. Increased muscle spindle feedback decreases admittance for lower frequencies which improves position task performance, while the admittance around the eigenfrequency is increased which may result in oscillations which deteriorate performance. There is a trade-off between performance improvement for the frequencies below the eigenfrequency and the performance loss due to emerging oscillation at the eigenfrequency. In Fig. 7 the performance is given as a function of the position (k_p) and velocity (k_v) feedback gain in case of a white noise perturbation signal. The performance is only evaluated

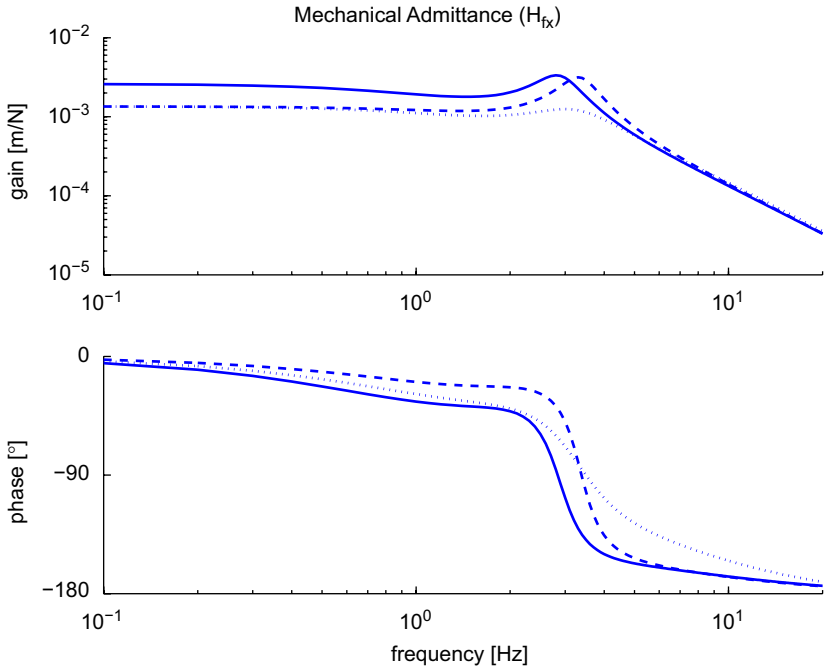

Fig. 4. FRF of the mechanical admittance of the joint, H_{fx}. The solid lines describe the system with the default parameter setting, see Table 2. With the dashed lines the muscle elasticity (k) is doubled; with the dotted lines both the muscle elasticity (k) and viscosity (b) are doubled.

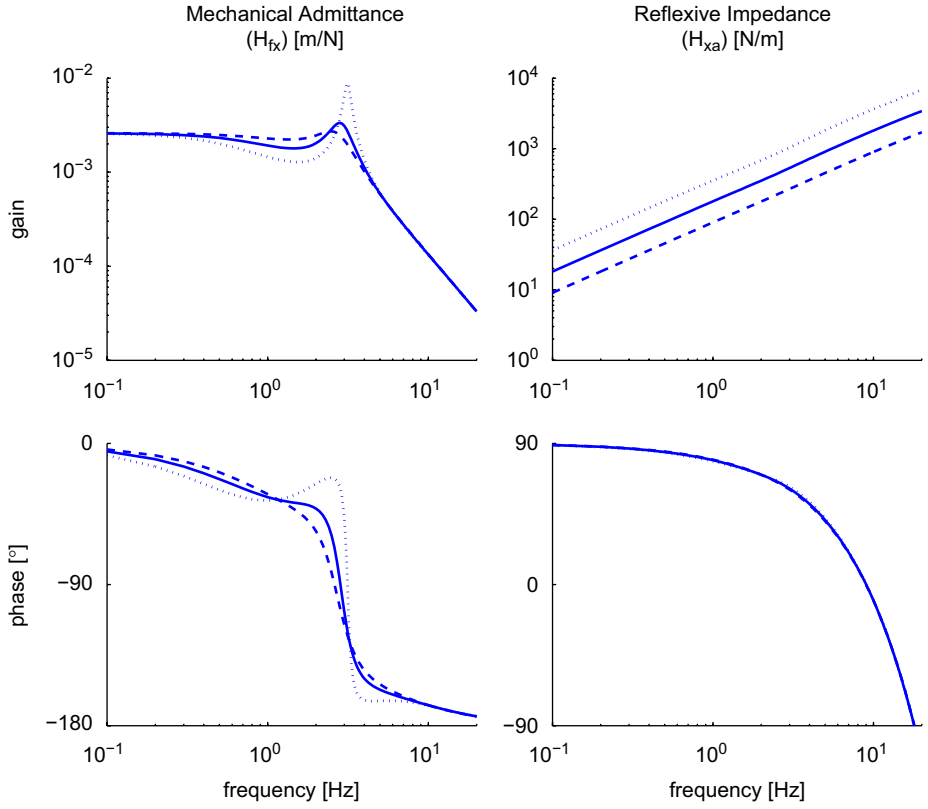

Fig. 5. Left: FRF of the mechanical admittance of the joint; right: FRF of the reflexive impedance. The solid lines describe the default system, see also Fig. 4. With the dashed lines afferent velocity feedback gain (k_v) is halved; with the dotted lines it is doubled.

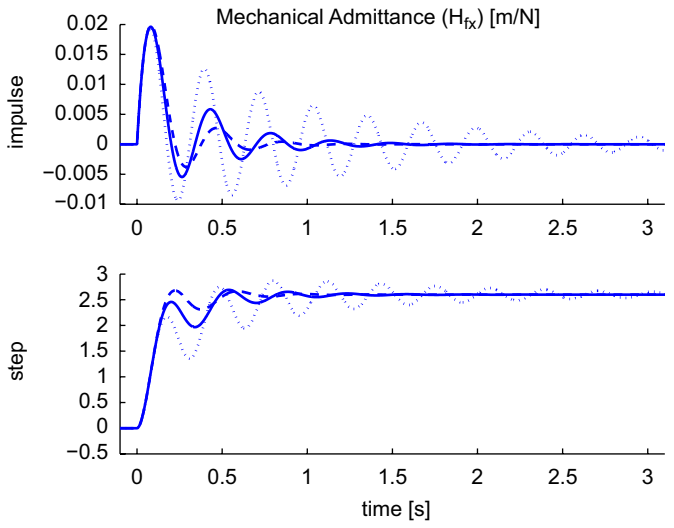

Fig. 6. Impulse response (upper) and step response (lower) of the mechanical admittance of the joint. Same settings as in Fig. 5.

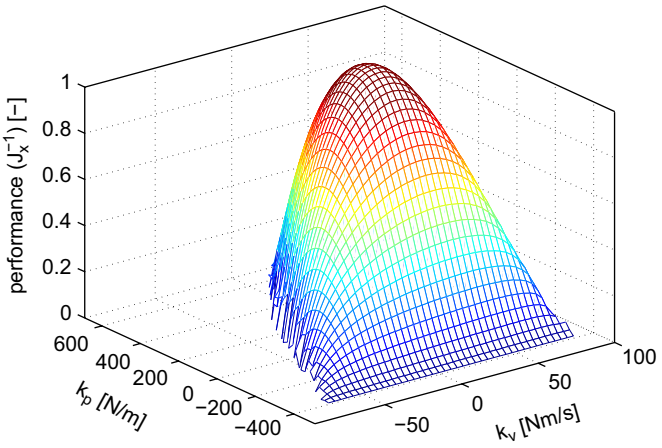

Fig. 7. Performance (J_x^{-1}) as a function of afferent position feedback (k_p) and afferent velocity feedback (k_v); normalized with respect to $k_v = 30\,\mathrm{Nm/s}$ and $k_p = 0\,\mathrm{N/m}$; higher values denote improved performance. Only parameter settings which result in a stable system are shown.

for parameter combinations resulting in a stable system. For the given conditions, a k_v of 18 Ns/m and a k_p of 117 N/m results in optimal performance. A 10% performance improvement is made compared to the default values of 30 Ns/m and 0 N/m. The relatively flat shape of the performance in the optimum indicates that it is robust to parameter variations.

3.2.2. Golgi tendon organ feedback

Fig. 8 displays the effect of force feedback from Golgi tendon organs. With force feedback the admittance decreases for the frequencies around the eigenfrequency and increases for lower frequencies. These two effects can be explained with Eq. (2): (1) increased bandwidth of both the intrinsic and afferent feedback pathway (H_{filtgto}) and

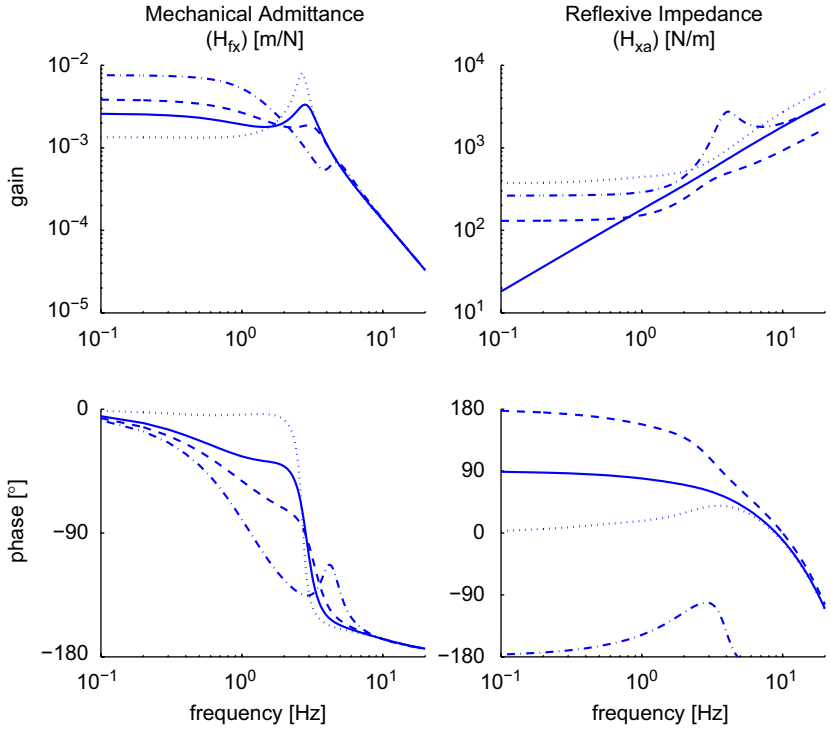

Fig. 8. Left: FRF of the mechanical admittance of the joint; right: FRF of the reflexive impedance. The solid lines describe the default system. With the dashed lines afferent force feedback gain (k_f) is set to 0.5; with the dash-dotted lines to 2 and with the dotted lines to −0.5.

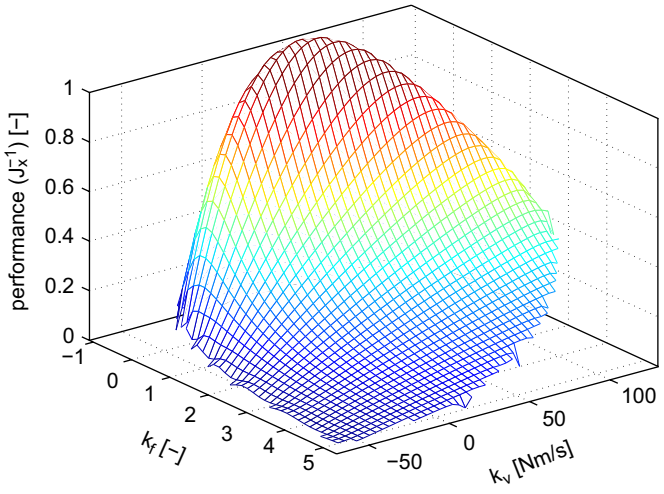

Fig. 9. Performance (J_x^{-1}) as a function of afferent force feedback (k_f) and afferent velocity feedback (k_v); normalized with respect to $k_v = 30\,\mathrm{Nm/s}$, $k_p = 117\,\mathrm{N/m}$ and $k_f = 0$; higher values denote improved performance. Only parameter settings which result in a stable system are shown.

(2) the effect on the muscle visco-elasticity ($-H_{ce}H_{gto}$). When force feedback becomes large ($k_f \approx 2$) oscillations occur around 6 Hz.

3.2.3. *Interaction between muscle spindle and Golgi tendon organ feedback*

In Fig. 9 the performance is given as a function of force (k_f) and velocity (k_v) feedback with the position feedback gain (k_p) set to 117 N/m. For these conditions the optimal force feedback gain is 0.35 and the optimal velocity feedback gain is 33 Ns/m, improving the performance by 14%. The optimum is less robust compared to the $k_p - k_v$ optimum and especially sensitive to variations in the force feedback gain.

4. Discussion

The presented neuromuscular control (NMC) model allows for analysis of the contributions of the separate components of the human motor system to the overall joint dynamics. The model includes afferent feedback of muscle spindles and Golgi tendon organs, as well as muscle properties as visco-elasticity of the contractile element and tendon elasticity. All these mechanisms interact and only by including all relevant physiological mechanisms and analyzing them in this holistic way an understanding of their interaction can be developed. In general it can be concluded that increased muscle co-activation decreases admittance (i.e. increases joint stiffness) and increases stability margins. The drawback, however, is that muscle co-activation is very energy demanding as the muscles will be activated continuously. Afferent feedback can further increase performance, but the effectiveness is limited by the stability margins to prevent oscillations, which are inherent with time-delayed feedback. Furthermore as a result of the muscle activation dynamics afferent feedback is primarily efficient in the lower frequency range. In conclusion there is a delicate balance between intrinsic and afferent/reflexive feedback.

4.1. Applications

With the developed model the effect of the various physiological structures onto joint dynamics can be visualized. Its main application is educational, i.e. to analyze the effect of the various mechanisms on the mechanical behavior, like the functional contribution of afferent feedback. For this purpose the developed model is implemented in a Matlab graphical user interface (The Mathworks, Inc., Natick, MA), which is made freely available on the internet, see Appendix C (Schouten et al., 2006)

To investigate the effect of parameter variations with the described model an indication of the range of variations is desirable. The number of studies which quantified all parameters in one experiment is limited (e.g. Kearney et al., 1997; Zhang and Rymer, 1997; Mirbagheri et al., 2000; de Vlugt et al., 2002; Schouten et al., 2008b). Within one experimental condition, typically the standard deviation of the parameters over the subjects is around 10–30% of the average value. It is obvious that the variations in both the muscle visco-elasticity and afferent feedback gains between experimental conditions like task instruction ('relax' or 'maximally resist') can be several orders of magnitude (Schouten et al., 2008b). The variations between subjects are the smallest for the subject-specific parameters (limb inertia, muscle activation dynamics, neural time delays) which are only marginally influenced by experimental conditions. On the other hand the variations in muscle visco-elasticity and afferent feedback gains can be substantial and are highly dependent on experimental conditions.

Other applications are more experimental. The model can be used to fit experimentally obtained admittances to find the underlying physiological parameters. An example is to fit the model to data from experiments to determine the modulation of the afferent feedback gains with varying conditions and compare these with theoretically optimal parameter settings. With the model, one could even predict the optimal experimental outcomes beforehand, or design the optimal experimental condition to provoke strong reflex modulation, e.g. finding experimental conditions in which afferent feedback is very beneficial or just the opposite, where already small afferent feedback gains result in unstable behavior.

The model in the present paper is universal and can be used on any joint; the shoulder serves only as an example. Additional data sets are included for the wrist and ankle and additionally users can implement their own, see Appendix C. Another example of an interesting application is the comparison of different joints. Distal joints have longer pathways and therefore larger neural latencies. As shown in the present study the effectiveness of feedback is severely hampered by its time delays. This implicates that the balance between intrinsic and afferent feedback is different for distal and proximal joints and that the role of afferent feedback can be larger in more proximal joints, and on the other hand that parameter variations are more critical in distal joints.

Conflict of Interest Statement

There is no conflict of interest.

Appendix A. Supplementary data

Supplementary data associated with this article can be found in the online version at doi:10.1016/j.jbiomech.2008.03.014.

References

Bobet, J., Norman, R.W., 1990. Least-squares identification of the dynamic relation between the electromyogram and joint moment. Journal of Biomechanics 23, 1275–1276.

de Vlugt, E., Schouten, A.C., van der Helm, F.C.T., 2002. Adaptation of reflexive feedback during arm posture to different environments. Biological Cybernetics 87, 10–26.

Friedland, B., 1986. Control System Design: An Introduction to State-space Methods. McGraw-Hill Series in Electrical Engineering. Control Theory. McGraw-Hill, New York Bernard Friedland ill; 25 cm Includes indexes.

Hultborn, H., Illert, M., Nielsen, J., Paul, A., Ballegaard, M., Wiese, H., 1996. On the mechanism of the post-activation depression of the H-reflex in human subjects. Experimental Brain Research 108, 450–462.

Kearney, R.E., Hunter, I.W., 1983. System-identification of human triceps surae stretch reflex dynamics. Experimental Brain Research 51, 117–127.

Kearney, R.E., Hunter, I.W., 1984. System-identification of human stretch reflex dynamics—tibialis anterior. Experimental Brain Research 56, 40–49.

Kearney, R.E., Stein, R.B., Parameswaran, L., 1997. Identification of intrinsic and reflex contributions to human ankle stiffness dynamics. IEEE Transactions on Biomedical Engineering 44, 493–504.

Loeb, G.E., 1987. Hard lessons in motor control from the mammalian spinal-cord. Trends in Neurosciences 10, 108–113.

Mirbagheri, M.M., Barbeau, H., Kearney, R.E., 2000. Intrinsic and reflex contributions to ankle dynamic stiffness in human: variation with activation level and position. Experimental Brain Research 135, 423–436.

Nielsen, J.B., Crone, C., Hultborn, H., 2007. The spinal pathophysiology of spasticity—from a basic science point of view. Acta Physiologica 189, 171–180.

Olney, S.J., Winter, D.A., 1985. Predictions of knee and ankle moments of force in walking from EMG and kinematic data. Journal of Biomechanics 18, 9–20.

Potvin, J.R., Norman, R.W., McGill, S.M., 1996. Mechanically corrected EMG for the continuous estimation of erector spinae muscle loading during repetitive lifting. European Journal of Applied Physiology and Occupational Physiology 74, 119–132.

Rudomin, P., Schmidt, R.F., 1999. Presynaptic inhibition in the vertebrate spinal cord revisited. Experimental Brain Research 129, 1–37.

Schouten, A.C., de Vlugt, E., van der Helm, F.C.T., Brouwn, G.G., 2001. Optimal posture control of a musculo-skeletal arm model. Biological Cybernetics 84, 143–152.

Schouten, A.C., de Vlugt, E., van Hilten, J.J.B., van der Helm, F.C.T., 2006. Design of a torque-controlled manipulator to analyse the admittance of the wrist joint. Journal of Neuroscience Methods 154, 134–141.

Schouten, A.C., de Vlugt, E., van der Helm, F.C.T., 2008a. Design of perturbation signals for the estimation of proprioceptive reflexes. IEEE Transactions on Biomedical Engineering 55, 1612–1619.

Schouten, A.C., de Vlugt, E., van Hilten, J.J., van der Helm, F.C.T., 2008b. Quantifying proprioceptive reflexes during position control of the human arm. IEEE Transactions on Biomedical Engineering 55, 311–321.

Sinkjaer, T., Toft, E., Andreassen, S., Hornemann, B.C., 1988. Muscle-stiffness in human ankle dorsiflexors—intrinsic and reflex components. Journal of Neurophysiology 60, 1110–1121.

Stein, R.B., Capaday, C., 1988. The modulation of human reflexes during functional motor-tasks. Trends in Neurosciences 11, 328–332.

Stein, R.B., Kearney, R.E., 1995. Nonlinear behavior of muscle reflexes at the human ankle joint. Journal of Neurophysiology 73, 65–72.

Stroeve, S., 1999. Impedance characteristics of a neuromusculoskeletal model of the human arm. I. Posture control. Biological Cybernetics 81, 475–494.

van der Helm, F.C.T., Schouten, A.C., de Vlugt, E., Brouwn, G.G., 2002. Identification of intrinsic and reflexive components of human arm dynamics during postural control. Journal of Neuroscience Methods 119, 1–14.

Voigt, M., Sinkjaer, T., 1998. The H-reflex in the passive human soleus muscle is modulated faster than predicted from post-activation depression. Brain Research 783, 332–346.

Zhang, L.Q., Rymer, W.Z., 1997. Simultaneous and nonlinear identification of mechanical and reflex properties of human elbow joint muscles. IEEE Transactions on Biomedical Engineering 44, 1192–1209.